





Communication

The Photochemical Stability of PbI₂ and PbBr₂: Optical and XPS and DFT Studies

Ivan S. Zhidkov ^{1,2,*} , Azat F. Akbulatov ³ , Alexander I. Poteryaev ^{1,2}, Andrey I. Kukharenko ^{1,2}, Alexandra V. Rasmetyeva ¹, Lyubov A. Frolova ³, Pavel A. Troshin ³  and Ernst Z. Kurmaev ^{1,2} 

¹ Institute of Physics and Technology, Ural Federal University, Mira 19 Street, Yekaterinburg 620002, Russia

² M. N. Mikheev Institute of Metal Physics of Ural Branch of Russian Academy of Sciences,

S. Kovalevskoi 18 Street, Yekaterinburg 620108, Russia

³ Federal Research Center of Problems of Chemical Physics and Medicinal Chemistry, Russian Academy of Sciences, Academician Semenov Avenue 1, Moscow Region, Chernogolovka 142432, Russia

* Correspondence: i.s.zhidkov@urfu.ru

Abstract: We investigated the photochemical stability of PbX₂ (X = I and Br) halides by optical and X-ray photoelectron spectroscopy (XPS). The optical absorbance displayed a strong reduction for PbI₂ with light soaking and permanent behavior for PbBr₂. The XPS survey spectra showed a sharp drop in the I:Pb ratio for PbI₂ from 1.63 to 1.14 with exposure time from 0 to 1000 h while for PbBr₂, it remains practically unchanged (1.59–1.55). The measurements of the XPS Pb 4f and Pb 5d spectra have shown the partial photolysis of PbI₂ with the release of metallic lead whereas PbBr₂ demonstrated remarkable photochemical stability. According to the density functional theory (DFT), calculations of the metal and iodide vacancy formation energies for PbBr₂ are higher than for PbI₂ which confirms the better stability to light soaking. The high photochemical stability of PbBr₂ means that it can be used as excess under MAPbBr₃ perovskite synthesis to improve not only the power conversion efficiency but also stability to light soaking.

Keywords: XPS; DFT; hybrid perovskite; stability; lead bromide



Citation: Zhidkov, I.S.;

Akbulatov, A.F.; Poteryaev, A.I.;

Kukharenko, A.I.; Rasmetyeva, A.V.;

Frolova, L.A.; Troshin, P.A.;

Kurmaev, E.Z. The Photochemical Stability of PbI₂ and PbBr₂: Optical and XPS and DFT Studies. *Coatings* **2023**, *13*, 784. <https://doi.org/10.3390/coatings13040784>

Academic Editor: Tongtong Xuan

Received: 23 March 2023

Revised: 10 April 2023

Accepted: 13 April 2023

Published: 18 April 2023



Copyright: © 2023 by the authors. Licensee MDPI, Basel, Switzerland. This article is an open access article distributed under the terms and conditions of the Creative Commons Attribution (CC BY) license (<https://creativecommons.org/licenses/by/4.0/>).

1. Introduction

Lead halide perovskites are considered the most promising materials for photovoltaics [1–3]. The power conversion efficiency (PCE) of perovskite solar cells has rapidly increased from 3.8 to 25.6% [4–6] and has reached the level of silicon cells. On the other hand, the low resistance of halide perovskites to light, temperature, and humidity hinders their commercialization [7]. To solve this problem, numerous studies have been performed over the last years to analyze the causes and mechanism of degradation of halide perovskites. Based on these studies, the main efforts have been directed at improving the surface morphology [8], grain size [9], halogen ratio [10], the composition of cations [11], charge transport layers [12,13], and electrodes [14,15]. It is found that the introduction of excess PbI₂ into CH₃NH₃PbI₃ (MAPbI₃) precursors reduced the defect density and increased the carrier lifetime and efficiency in a thin PbI₂-rich perovskite film [16–18]. Time resolved photoluminescence (TRPL) measurements have shown that excess PbI₂ results in a longer carrier lifetime in MAPbI₃ [19,20]. Scanning electron microscopy (SEM) and (X-ray diffraction) XRD measurements showed that the addition of a 10 mol % excess of PbI₂ to MAPbI₃ did not lead to obvious changes in morphology and crystal structure but was accompanied by a significant increase in PCE [16]. However, subsequent studies have shown that despite the benefits of increasing PCE, the implementation of excess PbI₂ does not improve the long-term photochemical stability of perovskites since simultaneously formed PbI₂ crystals easily decompose to metallic Pb and gaseous I₂ through photolysis [21–24]. In this regard, the search for other additives that perform the same useful role as excess PbI₂ but without photolysis is relevant and in demand [25]. One of these additives can be

PbBr₂, which like PbI₂ passivates the defects at grain boundaries and interfaces improving the quality of perovskite films [26–28]. It was found in Ref. [29] that if MAPbI₃ perovskite films decomposed with the formation of PbI₂ upon irradiation with visible light, then the introduction of PbBr₂ into a mixed halide solid solution caused more structural defects and grain boundaries and an increased defect density ensured the photochemical stability of these perovskite materials. In connection with this, we have undertaken a comparative study of the photochemical degradation of PbI₂ and PbBr₂ with the help of X-ray photoelectron spectroscopy (XPS) which has proven itself in the study of the resistance of halide perovskites currents to light soaking [30].

2. Experimental and Calculation Details

The PbI₂ precursor solution was prepared by adding 1.35 M PbI₂ in 1 mL anhydrous dimethyl sulfoxide (DMSO) (Sigma-Aldrich, Taufkirchen, Germany) and stirring at 60 °C for 12 h after which 7.5 mg of 2-TC Am was added to the precursor solution and then centrifuged at 4000 × g rpm min for 30 s. The spin-coating films were annealed at 70 °C on a hot plate for 5 min. The successful formation of PbI₂ and PbBr₂ films was examined by X-ray diffraction study (XRD) (Billerica, MA, USA). Only peaks of lead halides were detected (Figure 1), which indicates the high quality of the original films.

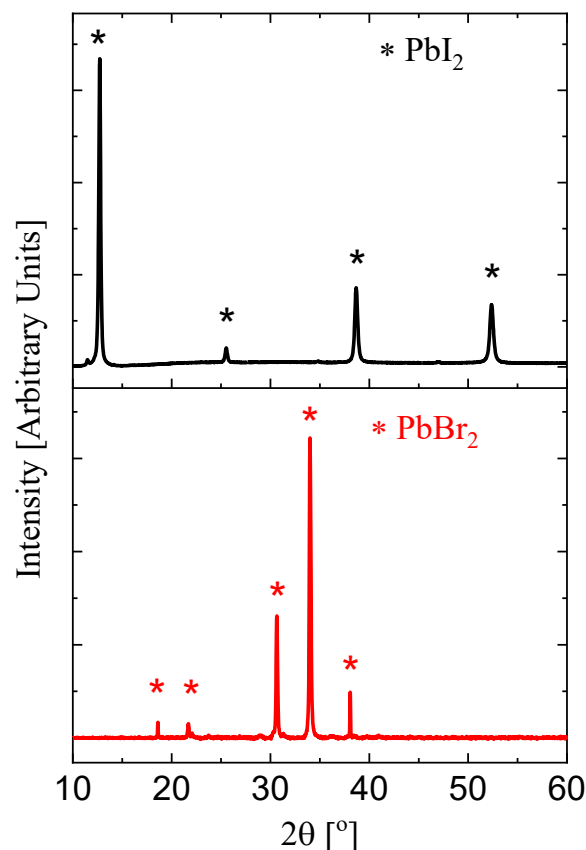


Figure 1. XRD of films under study: PbI₂—upper panel, PbBr₂—lower panel.

For photochemical aging, an LG sulfur plasma lamp (LG, Seoul, Republic of Korea) was used as a light source which provides a good approximation to the AM1.5G solar spectrum. Wavelengths below 350 nm were cutoff using an additional UV filter. The light power on the samples was ~70 mW/cm² at a temperature of 45 ± 2 °C. The absorption spectra were measured with an AvaSpec-2048-2 UV-VIS fiber spectrometer built into the glove box.

XPS was used to measure core level and VB spectra with the assistance of a PHI XPS 5000 VersaProbe spectrometer (ULVAC-Physical Electronics, Chanhassen, MN, USA)

equipped with a spherical quartz monochromator and an energy analyzer working in the range of binding energies from 0 to 1500 eV. The energy resolution was $\Delta E \leq 0.5$ eV.

The first principles calculations were carried out with the Vienna Ab initio Simulation Package [31,32]. The generalized gradient approximation was chosen in the PBE parametrization [33]. For an accurate calculation of the total energies and forces, the kinetic energy cutoff for the plane waves was set to 500 eV. The total energy convergence was set to 10^{-5} eV and atomic positions were relaxed with force convergence of 0.01 eV/Å per atom. The Monkhorst–Pack k point mesh of $2 \times 2 \times 1$ divided the reciprocal space.

3. Results and Discussion

The photochemical degradation of PbI_2 and PbBr_2 films was studied with the help of optical spectroscopy. The obtained absorption spectra of PbI_2 films irradiated for different times are compared with the spectra of PbBr_2 (Figure 2a,b). From the data obtained, it follows that after 200 h of irradiation, a significant decrease in the optical absorption of PbI_2 is observed; this indicates the photochemical degradation of this halide. This causes the film to decompose into Pb^0 and iodine gas, thereby reducing the film thickness and hence the absorption. On the other hand, the optical spectra of PbBr_2 show no change until 1000 h of exposure to visible light.

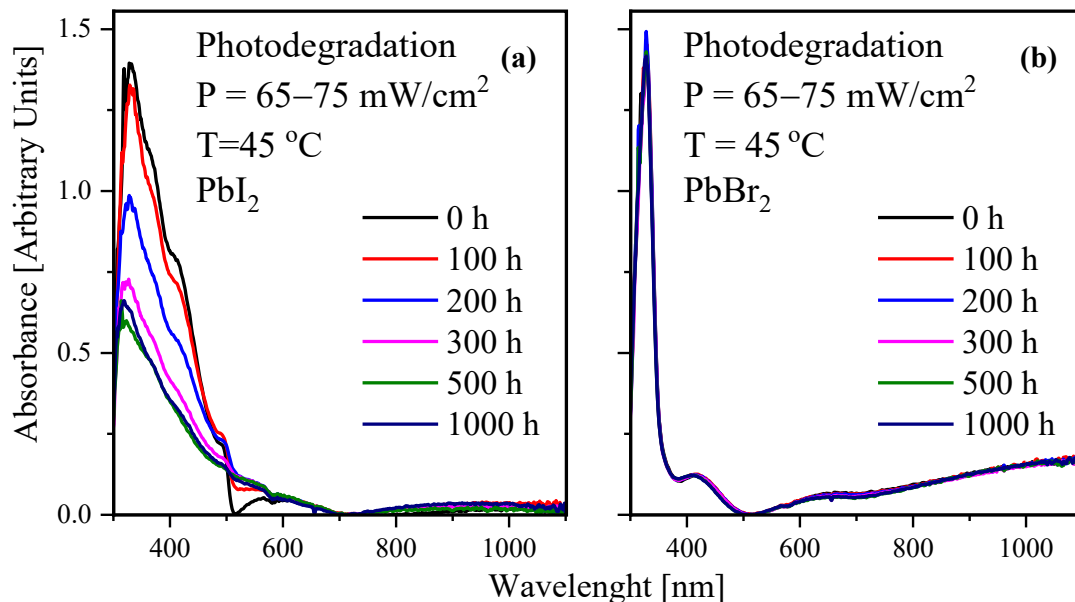


Figure 2. Optical absorbance of light-soaked PbI_2 (a) and PbBr_2 (b).

In Figure 3, the XPS survey spectra of PbI_2 and PbBr_2 halides irradiated with visible light are presented. Table 1 shows the surface composition determined from these spectra. As follows from these data, the I:Pb ratio drops sharply for PbI_2 from 1.63 to 1.14 with exposure time from 0 to 1000 h, while for PbBr_2 it remains practically unchanged (1.59–1.55). Such a reduction in the I:Pb ratio is usually associated with the photolysis of lead iodide which is accompanied by decomposition into metal and gaseous iodine. For a more complete analysis of the photolysis process, we measured the XPS Pb 4f and Pb 5d spectra of the core levels of PbI_2 and PbBr_2 as a function of the irradiation dose with a high energy resolution which is presented in Figure 3. For comparison, the spectra of metallic lead taken from [34] are shown in this figure. Their analysis shows that the contribution of metallic lead to the PbI_2 halide consistently increases with exposure time, which indicates an increase in the corresponding decay product and is in complete agreement with the results of measurements of XPS survey spectra. On the other hand, as follows from Figure 4, no traces of the appearance of metallic lead are observed when PbBr_2 halide is irradiated for 1000 h which again coincides with the invariance of the I:Br ratio determined from the XPS

survey spectra. Thus, the data obtained show a significant difference in the photochemical stability of PbI_2 and PbBr_2 binary halides and make it possible to justify the choice of an excess of PbBr_2 in the synthesis of halide perovskites as having a much higher resistance to photolysis.

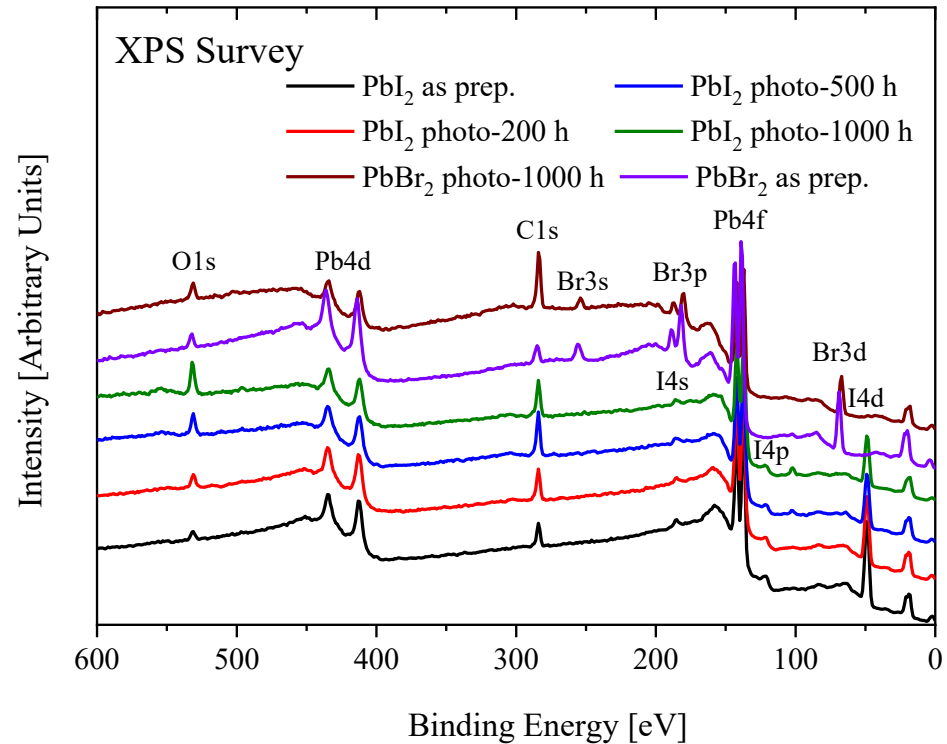


Figure 3. XPS survey spectra of PbI_2 and PbBr_2 halides after light-soaking.

Table 1. Surface composition (in at.%).

Sample	C	O	I	Br	Pb	Na	Ca	I(Br):Pb
PbI_2 as prepared	44.9	8.5	27.5	-	168	2.3	-	1.63
photo 200 h	53.4	11.0	20.3	-	15.3	-	-	1.32
photo 500 h	56.3	15.4	12.6	-	10.8	4.9	-	1.16
photo 1000 h	50.0	19.2	9.7	-	8.5	8.4	4.2	1.14
PbBr_2 as prepared	61.1	11.2	-	15.8	9.9	2.0	-	1.59
photo 1000 h	69.0	10.2	-	12.0	7.7	1.1	-	1.55

To demonstrate the relative stability of the PbBr_2 with respect to PbI_2 , we calculated the cohesive energy and defect formation energy of the PbBr_2 monolayer. For this aim, the monolayer with the $6 \times 6 \times 1$ supercell and vacuum size of 23 \AA was constructed for 1T PbBr_2 structure. The relaxed monolayer has a hexagonal honeycomb structure formed by the Br edge-sharing octahedra with parameters that are in good agreement with the earlier data of Ref. [35]. The Pb-Pb distance is 4.49 \AA and a monolayer thickness is 3.33 \AA , which assumes an octahedron squeezing along the direction perpendicular to the slab. The Pb-Br distance is 3.08 \AA and Br-Pb-Br angles are 93.6 and 86.4 for the Bromium atoms in the same and opposite Br surfaces, respectively.

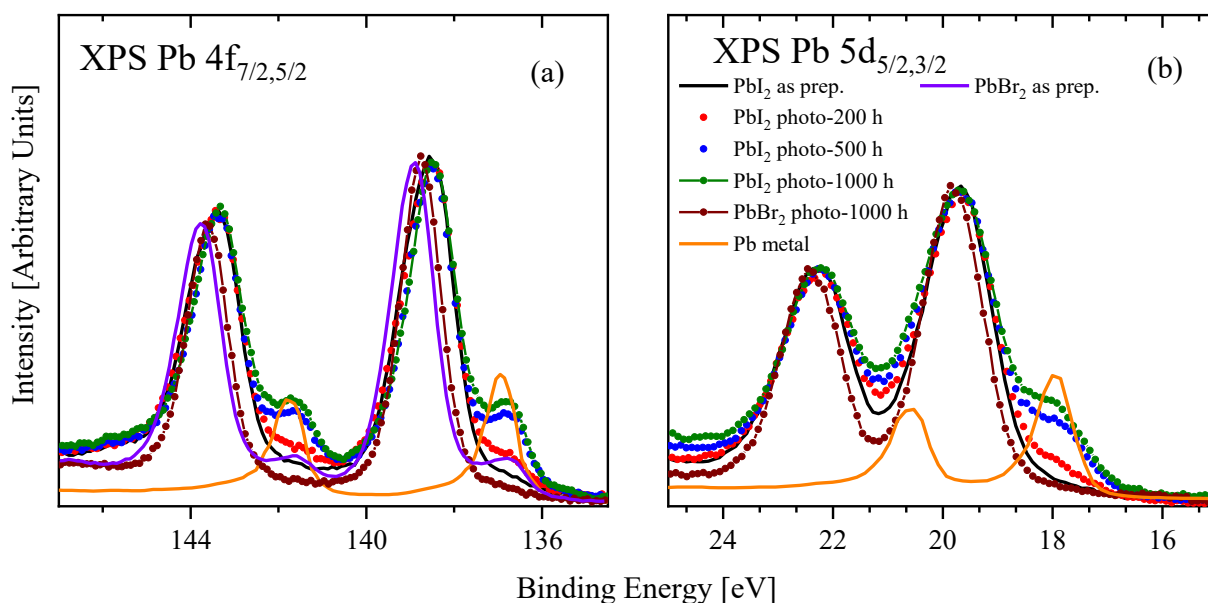


Figure 4. The comparison of high-energy resolved XPS Pb $4f_{7/2,5/2}$ (a) and Pb $5d_{5/2,3/2}$ (b) spectra of light-soaked halides and Pb-metal.

Figure 5 shows the relaxed crystal structures with the Pb and Br vacancies (left and right panels, respectively). In the V_{Pb} structure (Pb vacancy), the most distant from the vacant octahedron is almost unchanged: the Pb-Br distances deviate from ideal by the order of $m\text{\AA}$ and the angles are modified by less than half of a degree. This guarantees that the supercell size was properly chosen to minimize the vacancy interaction. The Pb- V_{Pb} distance is 4.36 \AA and the thickness of the monolayer in this place, 3.29 \AA , is about one percent smaller than in the ideal case. The V_{Pb} -Br distance is 3.2 \AA . Therefore, the lead atoms near the vacancy move to each other trying to close the hole but the surrounding Br_6 -octahedra are distorted in such a way that the Br-Br distance in the surface regular triangle is 4.76 \AA (this distance is 4.49 \AA in the pristine structure). In the case of the V_{Br} structure, the most distant octahedron is also almost unchanged with respect to the pristine structure. At the same time, the Pb-Pb distance for atoms close to the vacancy is 4.15 \AA , which is even smaller than the corresponding one in the V_{Pb} structure. The Br-Br distance in the surface regular triangle is 4.43 \AA , which is smaller not only with respect to the V_{Pb} structure but with a pristine one also. So, in the case of the V_{Br} structure, all atoms move towards the empty space created by Br vacancy.

The cohesive energy and defect formation energies of the Pb- and Br- vacancies (V_{Pb} and V_{Br}) were calculated as described in Refs. [36,37]. These results are presented in Table 2. We did not consider a charged defect since in the case of a charged slab, the total energy grows linearly with the distance from the slab; hence, it cannot be used to evaluate relative energies. The chemical potentials for the Br-rich and Pb-rich limits correspond to the Br_2 molecule and Pb bulk solid, respectively. The Br-poor and Pb-poor limits can be obtained from the formula for an equilibrium state for the compound under consideration,

$$\mu_{PbBr_2} = \mu_{Pb} + \mu_{Br_2}, \quad (1)$$

therefore, we take the values of the μ_{Br} from -3.04 eV to -1.5 eV and μ_{Pb} from -6.66 eV to -3.59 eV in the following discussions. One can clearly see that the all evaluated values for the $PbBr_2$ are larger than its corresponding PbI_2 counterparts [38]. These findings unambiguously indicate that $PbBr_2$ has higher stability with respect to the single vacancy formation of any type in comparison to the PbI_2 .

Table 2. The cohesive and defect formation energies in charge neutral state for the PbBr_2 compared to PbI_2 (from Wang et al. [38]). All values are in eV.

	1T PbBr_2			1T PbI_2		
	Pristine	V_{Pb}	V_{Br}	Pristine	V_{Pb}	V_{I}
E_{coh} , eV	3.07	2.95	2.99	2.63	2.59	2.62
E_{def} , Br/I-rich		1.2	2.3		1.1	2.2
E_{def} , Br/I-poor		4.3	1.3		4	0.9

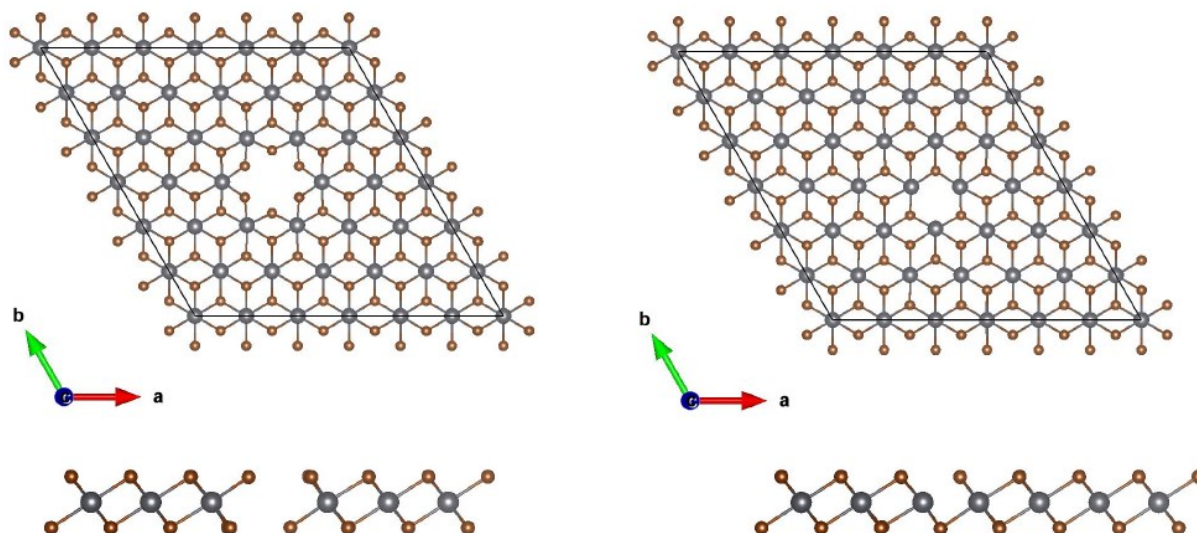


Figure 5. Left: top and side views of the Pb vacancy. Right: top and side views of Br vacancy. Pb and Br ions are shown by the grey and brown colours, respectively, a and b denotes crystal axes. The VESTA program was used for visualization [39].

Thus, the conducted experimental and theoretical studies show a much higher photochemical stability of PbBr_2 compared to PbI_2 halide. This suggests that PbBr_2 halide can be preferable for use as an excess additive for the improvement of properties of MAPbBr_3 perovskite.

4. Conclusions

The results of this work unambiguously indicate a significant photochemical degradation of lead iodide compared to lead bromide. It has been shown by XPS that significant degradation of PbI_2 starts already at 200 h, while PbBr_2 remains stable up to 1000 h of light soaking. In accordance with the DFT calculations, the formation energies of lead and halogen vacancies turn out to be higher in PbBr_2 than in PbI_2 , which confirms our experimental results. The obtained results indicate that the use of PbBr_2 as an excess additive in the development of stable hybrid organometallic perovskites is preferable.

Author Contributions: Conceptualization, E.Z.K. and P.A.T.; methodology, I.S.Z. and A.I.P.; formal analysis, I.S.Z., E.Z.K. and A.I.P.; investigation, I.S.Z., A.F.A., A.I.K., A.V.R., L.A.F. and A.I.P.; resources, I.S.Z. and P.A.T.; writing—original draft preparation, E.Z.K., A.I.P. and I.S.Z.; writing—review and editing, A.F.A., L.A.F., P.A.T. and A.I.P.; supervision, I.S.Z., P.A.T. and E.Z.K.; funding acquisition, I.S.Z., P.A.T. and A.I.P. All authors have read and agreed to the published version of the manuscript.

Funding: This work was supported by the Ministry of Science and Higher Education of the Russian Federation under the theme “Electron” No. AAAA-A18-118020190098-5 and Project FEUZ-2023-0013. The XPS measurements were supported by the Russian Foundation for Basic Research (Project No. 21-52-52002). Sample preparation was supported at FRC PCP MC RAS by the Ministry of Science and Higher Education of the Russian Federation (Project No. 0089-2019-0010/AAAA-A19-119071190044-3).

Institutional Review Board Statement: Not applicable.

Informed Consent Statement: Not applicable.

Data Availability Statement: Data is contained within the article.

Conflicts of Interest: The authors declare no conflict of interest.

References

1. Kalaiselvi, C.R.; Muthukumarasamy, N.; Velauthapillai, D.; Kang, M.; Senthil, T.S. Importance of Halide Perovskites for next Generation Solar Cells—A Review. *Mater. Lett.* **2018**, *219*, 198–200. [[CrossRef](#)]
2. Rosales, B.A.; Hanrahan, M.P.; Boote, B.W.; Rossini, A.J.; Smith, E.A.; Vela, J. Lead Halide Perovskites: Challenges and Opportunities in Advanced Synthesis and Spectroscopy. *ACS Energy Lett.* **2017**, *2*, 906–914. [[CrossRef](#)]
3. Huang, Y.-T.; Kavanagh, S.R.; Scanlon, D.O.; Walsh, A.; Hoye, R.L.Z. Perovskite-Inspired Materials for Photovoltaics and beyond—From Design to Devices. *Nanotechnology* **2021**, *32*, 132004. [[CrossRef](#)] [[PubMed](#)]
4. Kojima, A.; Teshima, K.; Shirai, Y.; Miyasaka, T. Organometal Halide Perovskites as Visible-Light Sensitizers for Photovoltaic Cells. *J. Am. Chem. Soc.* **2009**, *131*, 6050–6051. [[CrossRef](#)] [[PubMed](#)]
5. Jeong, J.; Kim, M.; Seo, J.; Lu, H.; Ahlawat, P.; Mishra, A.; Yang, Y.; Hope, M.A.; Eickemeyer, F.T.; Kim, M.; et al. Pseudo-Halide Anion Engineering for α -FAPbI₃ Perovskite Solar Cells. *Nature* **2021**, *592*, 381–385. [[CrossRef](#)]
6. Jiang, Q.; Zhao, Y.; Zhang, X.; Yang, X.; Chen, Y.; Chu, Z.; Ye, Q.; Li, X.; Yin, Z.; You, J. Surface Passivation of Perovskite Film for Efficient Solar Cells. *Nat. Photonics* **2019**, *13*, 460–466. [[CrossRef](#)]
7. Zhang, D.; Li, D.; Hu, Y.; Mei, A.; Han, H. Degradation Pathways in Perovskite Solar Cells and How to Meet International Standards. *Commun. Mater.* **2022**, *3*, 58. [[CrossRef](#)]
8. Jäger, M.; Teker, A.; Mannhart, J.; Braun, W. Independence of Surface Morphology and Reconstruction during the Thermal Preparation of Perovskite Oxide Surfaces. *Appl. Phys. Lett.* **2018**, *112*, 111601. [[CrossRef](#)]
9. Li, P.; Liang, C.; Bao, B.; Li, Y.; Hu, X.; Wang, Y.; Zhang, Y.; Li, F.; Shao, G.; Song, Y. Inkjet Manipulated Homogeneous Large Size Perovskite Grains for Efficient and Large-Area Perovskite Solar Cells. *Nano Energy* **2018**, *46*, 203–211. [[CrossRef](#)]
10. Oishi, Y.; Shimoda, M.; Narita, T.; Sakaguchi, K.; Era, M. Color-Tunable Langmuir Film with Layered Perovskite Structure by Controlling the Composition Ratio of Halogen Species. *Chem. Lett.* **2016**, *45*, 1418–1420. [[CrossRef](#)]
11. Hu, C.; Bai, Y.; Xiao, S.; Zhang, T.; Meng, X.; Ng, W.K.; Yang, Y.; Wong, K.S.; Chen, H.; Yang, S. Tuning the A-Site Cation Composition of FA Perovskites for Efficient and Stable NiO-Based p–i–n Perovskite Solar Cells. *J. Mater. Chem. A* **2017**, *5*, 21858–21865. [[CrossRef](#)]
12. Pandey, K.; Singh, D.; Gupta, S.K.; Yadav, P.; Sonvane, Y.; Lukačević, I.; Kumar, M.; Kumar, M.; Ahuja, R. Improving Electron Transport in the Hybrid Perovskite Solar Cells Using CaMnO₃-Based Buffer Layer. *Nano Energy* **2018**, *45*, 287–297. [[CrossRef](#)]
13. Hu, Z.; Chen, D.; Yang, P.; Yang, L.; Qin, L.; Huang, Y.; Zhao, X. Sol-Gel-Processed Yttrium-Doped NiO as Hole Transport Layer in Inverted Perovskite Solar Cells for Enhanced Performance. *Appl. Surf. Sci.* **2018**, *441*, 258–264. [[CrossRef](#)]
14. Kranthiraja, K.; Parashar, M.; Mehta, R.K.; Aryal, S.; Tamsal, M.; Kaul, A.B. Stability and Degradation in Triple Cation and Methyl Ammonium Lead Iodide Perovskite Solar Cells Mediated via Au and Ag Electrodes. *Sci. Rep.* **2022**, *12*, 18574. [[CrossRef](#)]
15. Rivkin, B.; Fassl, P.; Sun, Q.; Taylor, A.D.; Chen, Z.; Vaynzof, Y. Effect of Ion Migration-Induced Electrode Degradation on the Operational Stability of Perovskite Solar Cells. *ACS Omega* **2018**, *3*, 10042–10047. [[CrossRef](#)]
16. Jiang, M.; Wu, Y.; Zhou, Y.; Wang, Z. Observation of Lower Defect Density Brought by Excess PbI₂ in CH₃NH₃PbI₃ Solar Cells. *AIP Adv.* **2019**, *9*, 085301. [[CrossRef](#)]
17. Ma, Z.; Huang, D.; Liu, Q.; Yan, G.; Xiao, Z.; Chen, D.; Zhao, J.; Xiang, Y.; Peng, C.; Li, H.; et al. Excess PbI₂ Evolution for Triple-Cation Based Perovskite Solar Cells with 21.9% Efficiency. *J. Energy Chem.* **2022**, *66*, 152–160. [[CrossRef](#)]
18. Chen, L.; Chen, J.; Wang, C.; Ren, H.; Luo, Y.-X.; Shen, K.-C.; Li, Y.; Song, F.; Gao, X.; Tang, J.-X. High-Light-Tolerance PbI₂ Boosting the Stability and Efficiency of Perovskite Solar Cells. *ACS Appl. Mater. Interfaces* **2021**, *13*, 24692–24701. [[CrossRef](#)]
19. Roldán-Carmona, C.; Gratia, P.; Zimmermann, I.; Grancini, G.; Gao, P.; Graetzel, M.; Nazeeruddin, M.K. High Efficiency Methylammonium Lead Triiodide Perovskite Solar Cells: The Relevance of Non-Stoichiometric Precursors. *Energy Environ. Sci.* **2015**, *8*, 3550–3556. [[CrossRef](#)]
20. Cao, D.H.; Stoumpos, C.C.; Malliakas, C.D.; Katz, M.J.; Farha, O.K.; Hupp, J.T.; Kanatzidis, M.G. Remnant PbI₂, an Unforeseen Necessity in High-Efficiency Hybrid Perovskite-Based Solar Cells? *APL Mater.* **2014**, *2*, 091101. [[CrossRef](#)]
21. Park, B.; Kedem, N.; Kulbak, M.; Lee, D.Y.; Yang, W.S.; Jeon, N.J.; Seo, J.; Kim, G.; Kim, K.J.; Shin, T.J.; et al. Understanding How Excess Lead Iodide Precursor Improves Halide Perovskite Solar Cell Performance. *Nat. Commun.* **2018**, *9*, 3301. [[CrossRef](#)] [[PubMed](#)]
22. Roose, B.; Dey, K.; Chiang, Y.-H.; Friend, R.H.; Stranks, S.D. Critical Assessment of the Use of Excess Lead Iodide in Lead Halide Perovskite Solar Cells. *J. Phys. Chem. Lett.* **2020**, *11*, 6505–6512. [[CrossRef](#)] [[PubMed](#)]
23. The Photodecomposition of Lead Iodide. *Proc. R. Soc. Lond. Ser. A Math. Phys. Sci.* **1965**, *284*, 272–288. [[CrossRef](#)]
24. Tumen-Ulzii, G.; Qin, C.; Klotz, D.; Leyden, M.R.; Wang, P.; Auffray, M.; Fujihara, T.; Matsushima, T.; Lee, J.; Lee, S.; et al. Detrimental Effect of Unreacted PbI₂ on the Long-Term Stability of Perovskite Solar Cells. *Adv. Mater.* **2020**, *32*, 1905035. [[CrossRef](#)] [[PubMed](#)]

25. Cheng, F.; Zhang, J.; Pauporté, T. Chlorides, Other Halides, and Pseudo-Halides as Additives for the Fabrication of Efficient and Stable Perovskite Solar Cells. *ChemSusChem* **2021**, *14*, 3665–3692. [[CrossRef](#)]
26. Zhang, J.; Li, X.; Wang, L.; Yu, J.; Wageh, S.; Al-Ghamdi, A.A. Enhanced Performance of CH₃NH₃PbI₃ Perovskite Solar Cells by Excess Halide Modification. *Appl. Surf. Sci.* **2021**, *564*, 150464. [[CrossRef](#)]
27. Fang, X.; Zhang, K.; Li, Y.; Yao, L.; Zhang, Y.; Wang, Y.; Zhai, W.; Tao, L.; Du, H.; Ran, G. Effect of Excess PbBr₂ on Photoluminescence Spectra of CH₃NH₃PbBr₃ Perovskite Particles at Room Temperature. *Appl. Phys. Lett.* **2016**, *108*, 071109. [[CrossRef](#)]
28. Sheikh, M.A.K.; Singh, S.; Abdur, R.; Lee, S.-M.; Kim, J.-H.; Nam, H.-S.; Lee, H.; Lee, J. Effects of the PbBr₂:PbI₂ Molar Ratio on the Formation of Lead Halide Thin Films, and the Ratio's Application for High Performance and Wide Bandgap Solar Cells. *Materials* **2022**, *15*, 837. [[CrossRef](#)]
29. Misra, R.K.; Ciammaruchi, L.; Aharon, S.; Mogilyansky, D.; Etgar, L.; Visoly-Fisher, I.; Katz, E.A. Effect of Halide Composition on the Photochemical Stability of Perovskite Photovoltaic Materials. *ChemSusChem* **2016**, *9*, 2572–2577. [[CrossRef](#)]
30. Zhidkov, I.S.; Boukhvalov, D.W.; Akbulatov, A.F.; Frolova, L.A.; Finkelstein, L.D.; Kukharensko, A.I.; Cholakh, S.O.; Chueh, C.-C.; Troshin, P.A.; Kurmaev, E.Z. XPS Spectra as a Tool for Studying Photochemical and Thermal Degradation in APbX₃ Hybrid Halide Perovskites. *Nano Energy* **2021**, *79*, 105421. [[CrossRef](#)]
31. Kresse, G.; Furthmüller, J. Efficiency of Ab-Initio Total Energy Calculations for Metals and Semiconductors Using a Plane-Wave Basis Set. *Comput. Mater. Sci.* **1996**, *6*, 15–50. [[CrossRef](#)]
32. Kresse, G.; Furthmüller, J. Efficient Iterative Schemes for Ab Initio Total-Energy Calculations Using a Plane-Wave Basis Set. *Phys. Rev. B* **1996**, *54*, 11169–11186. [[CrossRef](#)]
33. Perdew, J.P.; Burke, K.; Ernzerhof, M. Generalized Gradient Approximation Made Simple. *Phys. Rev. Lett.* **1996**, *77*, 3865–3868. [[CrossRef](#)]
34. Rondon, S.; Sherwood, P.M.A. Core Level and Valence Band Spectra of Lead by XPS. *Surf. Sci. Spectra* **1998**, *5*, 83–89. [[CrossRef](#)]
35. Beral, A.; Bera, J.; Das, C.; Sahu, S. Prediction of Two Dimensional Wide Bandgap Semiconductor PbBr₂ Monolayer Using First Principle Calculations. In Proceedings of the 65th DAE Solid State Physics Symposium, Mumbai, India, 15–19 December 2021; pp. 598–599.
36. Freysoldt, C.; Grabowski, B.; Hickel, T.; Neugebauer, J.; Kresse, G.; Janotti, A.; Van de Walle, C.G. First-Principles Calculations for Point Defects in Solids. *Rev. Mod. Phys.* **2014**, *86*, 253–305. [[CrossRef](#)]
37. Van de Walle, C.G.; Neugebauer, J. First-Principles Calculations for Defects and Impurities: Applications to III-Nitrides. *J. Appl. Phys.* **2004**, *95*, 3851–3879. [[CrossRef](#)]
38. Wang, H.; Wang, X.; Li, D. Defects of Monolayer PbI₂: A Computational Study. *Phys. Chem. Chem. Phys.* **2021**, *23*, 20553–20559. [[CrossRef](#)]
39. Momma, K.; Izumi, F. VESTA 3 for Three-Dimensional Visualization of Crystal, Volumetric and Morphology Data. *J. Appl. Crystallogr.* **2011**, *44*, 1272–1276. [[CrossRef](#)]

Disclaimer/Publisher's Note: The statements, opinions and data contained in all publications are solely those of the individual author(s) and contributor(s) and not of MDPI and/or the editor(s). MDPI and/or the editor(s) disclaim responsibility for any injury to people or property resulting from any ideas, methods, instructions or products referred to in the content.